

# Summer Sea Ice Concentration, Motion, and Thickness Near Areas of Proposed Offshore Oil and Gas Development in the Canadian Beaufort Sea – 2009

RYAN J. GALLEY,<sup>1,2</sup> B.G.T. ELSE,<sup>1</sup> S.J. PRINSEBERG,<sup>3</sup> D. BABB<sup>1</sup> and D.G. BARBER<sup>1</sup>

*(Received 31 October 2011; accepted in revised form 24 May 2012)*

**ABSTRACT.** This study was motivated by the potential development of offshore oil exploration leases in the Canadian Southern Beaufort Sea, an area within the Inuvialuit Settlement Region. Sea ice concentration, extent, motion, and thickness data are vital to the success of potential oil operations in this region, and relevant data cannot be gleaned from larger-scale hemispheric studies. We therefore undertook regionally specific sea ice analyses in the southern Beaufort Sea during the summer drilling season (July, August, and September) in 2009 and over the long-term (1996–2010). On average, the Canadian oil lease areas contain mostly old sea ice during the drilling season and have not experienced significant decreasing trends in total or old sea ice. The average sea ice motion in the region for the period was anti-cyclonic at  $20\text{--}25\text{ cm}\cdot\text{s}^{-1}$ , acting to transport sea ice southward toward the lease areas. Summer 2009 was used as a case study of regional ice concentration, motion, and thickness and to compare September sea ice thickness measurements to data collected in April 2009. In the summer of 2009, old sea ice was the predominant ice type in the lease areas. Sea ice motion was anti-cyclonic and faster than the long-term average, reaching  $60\text{ cm}\cdot\text{s}^{-1}$  west of Banks Island and across the north end of the lease areas. September 2009 sea ice thickness (mean = 1.03 m,  $\sigma = 0.97\text{ m}$ ) was modal about the 0.20–0.29 m thickness bin. The sea ice thickness distribution was spatially variable, with the thickest ice occurring at the north end of the study area, in an area dominated by high old ice concentrations. Ice thicknesses greater than 10 m (the upper limit our instruments could measure) were encountered. Thinner sea ice predominated at the periphery of the core Beaufort Sea multi-year pack. Near the oil lease areas, the sea ice thickness distributions were shifted left on the histogram in comparison to those farther north, resulting in a greater proportion of relatively thick sea ice due to the thermodynamic loss of thinner ( $< 1.5\text{ m}$ ) first-year ice during its southward movement. After enduring a summer's melt, however, this thicker ice at the south end of the study region had thinned in comparison to the ice at the north end.

**Key words:** sea ice, ice concentration, ice extent, ice motion, ice thickness, Beaufort Sea, offshore oil exploration

**RÉSUMÉ.** La présente étude a été motivée par la mise en valeur potentielle des concessions d'exploration pétrolière au large de la mer de Beaufort, dans la partie sud canadienne, un endroit qui fait partie de la région désignée des Inuvialuit. Les données relatives à la concentration, à l'étendue, au déplacement et à l'épaisseur de la glace de mer sont essentielles à la réussite de l'exploitation éventuelle du pétrole dans cette région, et les données pertinentes ne peuvent être dépouillées à partir d'études hémisphériques réalisées à grande échelle. Par conséquent, nous avons entrepris de faire des analyses particulièrement régionales de la glace de mer du sud de la mer de Beaufort pendant la saison de forage d'été (juillet, août et septembre) en 2009 de même que sur une plus longue période (1996-2010). En moyenne, les régions visées par les concessions pétrolières canadiennes renferment principalement de la vieille glace de mer pendant la saison de forage, et elles n'enregistrent pas d'importantes tendances à la baisse sur le plan de l'ensemble de la glace de mer ou de la vieille glace de mer. Dans la région, le déplacement moyen de la glace de mer pendant la période était anticyclonique à  $20\text{--}25\text{ cm}\cdot\text{s}^{-1}$ , ce qui avait pour effet de transporter la glace de mer vers le sud et vers les concessions. L'été 2009 nous a servi d'étude de cas en matière de concentration, de déplacement et d'épaisseur de la glace régionale, et nous a permis de comparer les mesures de l'épaisseur de la glace de mer de septembre aux données recueillies en avril 2009. À l'été 2009, la vieille glace de mer représentait le type de glace prédominant dans les concessions. Le déplacement de la glace de mer était anticyclonique et se faisait plus vite que la moyenne à long terme, atteignant ainsi  $60\text{ cm}\cdot\text{s}^{-1}$  à l'ouest de l'île Banks et à la hauteur du nord de la zone de concessions. En septembre 2009, l'épaisseur de la glace de mer (moyenne = 1,03 m,  $\sigma = 0,97\text{ m}$ ) était modale à la hauteur de la classe de l'épaisseur 0,20–0,29 m. La répartition de l'épaisseur de la glace de mer variait en fonction de l'emplacement, la glace la plus épaisse se trouvant du côté nord de la région étudiée, dans une zone dominée par de fortes concentrations de vieille glace. La glace atteignait des épaisseurs de plus de 10 m (la limite maximale que nos instruments pouvaient mesurer) par endroits. Une glace de mer plus mince prédominait la périphérie du noyau de la banquise pluriannuelle de la mer de Beaufort. Près de la zone

<sup>1</sup> Centre for Earth Observation Science, University of Manitoba, 460 Wallace Building, 125 Dysart Road, Winnipeg, Manitoba R3T 2N2, Canada

<sup>2</sup> Corresponding author: galley@cc.umanitoba.ca

<sup>3</sup> Coastal Ocean Science, Bedford Institute of Oceanography, Fisheries and Oceans Canada, 1 Challenger Drive, PO Box 1006, Dartmouth, Nova Scotia B2Y 4A2, Canada

de concessions pétrolières, les répartitions d'épaisseurs de glace de mer se sont déplacées vers la gauche sur l'histogramme comparativement à celles plus au nord, ce qui a donné une plus grande proportion de glace de mer relativement épaisse en raison de la perte thermodynamique de la glace plus mince de première année ( $< 1,5$  m) pendant son déplacement vers le sud. Cependant, après avoir enduré la fonte d'un été, la glace plus épaisse du côté sud de la région à l'étude s'était amincie comparativement à la glace se trouvant du côté nord.

Mots clés : glace de mer, concentration de la glace, étendue de la glace, déplacement de la glace, épaisseur de la glace, mer de Beaufort, exploration pétrolière au large

Traduit pour la revue *Arctic* par Nicole Giguère.

## INTRODUCTION

Summer sea ice extent in the Northern Hemisphere has been on the decline since the late 1970s. In recent years, decreasing ice extent has renewed discussions of offshore oil and gas development in the Arctic that began in earnest in the 1970s. Oil and natural gas reserves are known to exist on the Mackenzie Shelf in the southern Beaufort Sea, and several petroleum companies have shown interest in their development (Northern Oil and Gas Branch, 2009). The United States Geological Survey (USGS) estimates that the Amerasian Basin (consisting of the Mackenzie Shelf and much of the southern Beaufort Sea in Canadian waters) contains 9.72 billion barrels of undiscovered oil, 57 000 billion cubic feet of natural gas, and 542 million barrels of natural gas liquids: a total of 19.7 billion barrels of oil equivalent (USGS World Energy Assessment Team, 2000; Gautier et al., 2009). The Northern Oil and Gas Branch's 2008 annual report (2009) estimates that 35% of Canada's light crude and 33% of Canada's natural gas in conventional accumulations are found in Canada's North. Many recently issued Canadian offshore exploration licenses in the Beaufort Sea expire in 2016 and 2017 (Northern Oil and Gas Branch, 2009), which has led to increased efforts towards biological and physical assessment of these areas (e.g., ArcticNet, 2009).

Despite negative trends in its extent, sea ice remains an important factor in the discussion of offshore oil and gas development in Canada's western Arctic. It is a principal hazard to drilling operations, which may include ice strengthened drill ships, ice-capable tankers, and icebreaker escorts. From an exploration standpoint, ice extent determines feasible drilling locations and the length of the open water season; ice thickness determines the ease with which a drill ship may be operated without interruption at an offshore well; stage of ice development is an important factor in ice strength and thus defines engineering requirements for drill ships and support vessels; and ice motion is important in forecasting how ice hazards advance to the drill site. Sea ice also provides a major impediment to cleaning up potential spills or leaks and further provides a mechanism of entrainment and transport of oil at the surface.

In the Beaufort Sea sector of the Arctic Ocean, summer sea ice extent varies greatly between years (Barnett, 1976, 1980; Drobot and Maslanik, 2003; Galley et al., 2008; Parkinson and Cavalieri, 2008). In a monthly regional analysis,

Meier et al. (2007) noted significant decreasing trends in sea ice extent in August ( $-2.6\%$  decade<sup>-1</sup>) and September ( $-9.6\%$  decade<sup>-1</sup>) for the period 1979–2006. Perovich and Richter-Menge (2009) compared the results of Meier et al. (2007) to those of Parkinson et al. (1999), whose trend analysis ended a decade earlier, and found that most trends showed an increased rate of decline. On the basis of a satellite-derived analysis of sea ice age, Maslanik et al. (2011) note that in the Canada Basin of the Arctic Ocean, multi-year sea ice coverage in March decreased by 83% from 2002 to 2009. However, these trend studies generalize the entire Beaufort Sea (e.g., Comiso and Nishio, 2008; Parkinson and Cavalieri, 2008; Maslanik et al., 2011), which consists of several distinct ice regimes (see e.g., Haas et al., 2010). For the oil lease regions in the Canadian Beaufort Sea, specific regional analyses of trends in ice extent are currently lacking.

Sea ice motion in the Beaufort Sea is an important consideration because of the unique regional interaction of the atmosphere and the sea ice and ocean surface in the region (e.g., Colony and Thorndike, 1984; Serreze et al., 1989; Kimura and Wakatsuchi, 2000; Rigor et al., 2002; Drobot and Maslanik, 2003; Overland, 2009). Annual average sea ice motion in the southern Beaufort Sea is characterized by the Beaufort Gyre (Vowinckel and Orvig, 1970), an anti-cyclonic (clockwise) feature of the ocean surface driven mainly by synoptic-scale atmospheric circulation (sea-level pressure highs) in the Canada Basin of the Arctic Ocean. A long-term sea level pressure climatology of the Beaufort Sea in summer shows that the semi-permanent Beaufort High does not occur year-round, but only in the fall and spring (Overland, 2009). Overland (2009) notes that the summer sea level pressure is fairly flat over the Beaufort in the long term (1979–2007), suggesting that on average over his study period, the surface conditions were controlled by the local heat and moisture balance and the presence of smaller local weather systems. Serreze and Barrett (2011), however, showed that the frequency of anti-cyclonic surface winds in the Beaufort Sea is fairly constant throughout the year. Summer rotation of the Beaufort Gyre has been the subject of recent studies which show that anti-cyclonic movement of the sea ice pack may slow down or even change to a cyclonic flow, especially in summer (e.g., Serreze et al., 1988; Preller and Posey, 1989; Lukovich and Barber, 2006; Asplin et al., 2009). Since 1997, however, the Beaufort Sea ocean currents and sea ice circulation

patterns have been closely coupled. They have been wind-driven in an anomalous anti-cyclonic fashion compared to the longer term (Overland, 2009), creating convergent conditions at the surface that increase sea ice concentration and ice thickness because of dynamic forces (Proshutinsky et al., 2002). Serreze and Barrett (2011) also note that the record summer sea ice loss in the Arctic in 2007 coincided with an unusually strong Beaufort Sea high in combination with unusually low pressure over Eurasia. Ogi et al. (2008) showed that southerly winds resulting from this pressure difference promoted ice transport away from the Siberian and Alaskan coasts, and Stroeve et al. (2007) concluded that strong melt resulted from unusually positive air temperature anomalies in the East Siberian and Chukchi Seas. The 2007 atmospheric pattern was enhanced by extensive coverage of younger first-year sea ice types, and a similar but less-developed atmospheric pattern prevailed in summer 2008 and most of the summer of 2009 (Serreze and Barrett, 2011). In general, sea ice velocity and vorticity in the Beaufort Gyre is related to ice concentration. In April, when ice concentrations are highest, velocity and vorticity are generally small and weak, while during August and September, when ice extent and concentration are lowest, velocity and vorticity in the sea icescape reach their annual maxima (Barry and Maslanik, 1989; Lukovich and Barber, 2006; Spreen et al., 2011).

Thickness is one of the most difficult sea ice parameters to measure on large scales, but there is evidence of a shift from a previous Arctic icescape dominated by thicker perennial sea ice to one dominated by thinner seasonal sea ice (Comiso, 2002; Nghiem et al., 2006; Kwok, 2007; Maslanik et al., 2007, 2011; Barber et al., 2009). In the Beaufort Sea, several observations of thinning ice (i.e., Rothrock et al., 1999; Melling and Riedel, 2004; Yu et al., 2004; Melling et al., 2005; Perovich et al., 2008) have been published in the last decade. Melling et al. (2005) showed reductions ( $-0.27$  m·decade<sup>-1</sup> and  $-0.07$  m·decade<sup>-1</sup>) in ice-only and ice-pack draft in the eastern Beaufort Sea between 1991 and 2003. Kwok et al. (2009) provided a five-year record (fall 2003 to spring 2008) of sea ice thickness and volume over the Arctic Ocean derived from Ice, Cloud and land Elevation Satellite (ICESat) campaigns in combination with QuikScat data showing the distribution of multi-year and first-year sea ice across the Northern Hemisphere. In their time series, Kwok et al. (2009) observed strong reductions in Arctic basin sea ice volume as multi-year ice was replaced by first- and second-year sea ice. Haas et al. (2010) also observed that the areal fraction of multi-year sea ice in this region decreased substantially following the September sea ice extent minimum of 2007, a fact highlighted by several studies (Perovich et al., 2008; Barber et al., 2009; Perovich and Richter-Menge, 2009). Synoptic sea ice thickness measurements carried out in April 2009 sampled what Haas et al. (2010) call the core of multi-year sea ice in the Beaufort Sea (Haas et al., 2010: Table 1 and Fig. 1) as it was advected south by the clockwise motion of the Beaufort Gyre. This core of multi-year sea ice in April had a mean thickness of

2.33–3.27 m, while the predominantly first-year ice just to the west had a mean thickness of only 1.11 m, making it amongst the thinnest ice they sampled in the entire Arctic (Haas et al., 2010). Evaluation of April 2009 sea ice thickness distributions in the Beaufort Sea revealed first-year sea ice had modes of 1.7–2.3 m, while second-year and multi-year sea ice had modes of 2.2 m and 3.0–3.4 m respectively (Haas et al., 2010). Finally, neither Kwok et al. (2009) nor Haas et al. (2010) observed any significant interannual decreases in first-year sea ice thickness; they concluded that sustained first-year sea ice thickness hinges on thickening as a result of deformation processes.

Here we provide a regional-scale analysis of sea ice conditions in the southern Beaufort Sea in summer, focusing on the areas where oil and gas exploration leases have been purchased. We calculate the average concentration of total sea ice and old sea ice for the expected summer drilling season over the period 1996 to 2010, and we investigate trends in those parameters. We also determine the typical sea ice motion for the area. Finally, we present sea ice thickness data collected in September 2009. These data, when compared with the Haas et al. (2010) measurements made in April 2009, provide a snapshot of regional and seasonal ice thickness and thinning. Overall, our analyses provide a comprehensive characterization of the sea ice conditions at a scale useful for decision making regarding oil and gas development in the newly established Beaufort Sea exploration leases and for the Beaufort Sea Regional Environmental Assessment (BREA). BREA is a Canadian government initiative designed to prepare for increased industrial development in the southern Beaufort Sea. It is vital that timely analysis be presented to ensure that levels of Canadian government, the Inuvialuit people of Canada's western Arctic, and industry are prepared for offshore resource exploration and development.

## METHODS

The Canadian southern Beaufort Sea east of 140° W, south of 75° N and bounded by the west coast of Banks Island in the east and the continental coast in the south (Fig. 1) is our area of interest because of the Canadian oil exploration licenses contained within it (Northern Oil and Gas Branch, 2009). The expected summer oil drilling season encompasses July, August, and September (JAS). This period covers ~100 days when sea ice concentrations in the southern Beaufort Sea are lowest in and around the oil lease areas (Drobot and Maslanik, 2003; Galley et al., 2008; CIS, 2010) while avoiding June and October, when sea ice conditions in the region are highly variable (Galley et al., 2008). A July to September sea ice climatology for the southern Beaufort Sea between 1996 and 2010 was created using the weekly Canadian Ice Service (CIS) digital archive to show the mean summer sea ice conditions in the regions and to calculate trends therein. Radarsat-1 SAR data have been the primary data source for the CIS archive for this period,

and the quality indices are high. Tivy et al. (2011) contains an extensive explanation of the suitability of these data for climatological and trend analyses. The CIS digital archive reports ice conditions on a weekly basis by defining polygons using the egg code. This egg code contains information on the total ice concentration (in tenths) and the partial concentrations of up to three predominant stages of development (in tenths) stored in ArcInfo interchange format. We converted the interchange format files to shapefiles in a Lambert Conformal Conic projection, using ArcView 3.2. The shapefile polygon data were converted to a two-by-two km grid using Matlab. The grids were then used to compute the average total, old, and first-year sea ice concentrations in July to September for each year. We then calculated the total, first-year, and old ice (a superset of second-year and multi-year sea ice) concentrations, as well as trends in those summer drilling season concentrations over the 1996–2010 time period, using least squares fit regression. The significance of each trend was tested using a standard F-test (Moore, 1995). The trend data were tested for normality and autocorrelation sufficiently low to allow for parametric analysis. Any trend with an associated  $p$  value of 0.05 or less was considered statistically significant (95% level).

To characterize regional ice motion, we used Polar Pathfinder daily 25 km EASE-Grid sea ice motion vectors derived from a combination of data from the International Arctic Buoy Program drifting buoys, using passive microwave (Scanning Multichannel Microwave Radiometer, or SMMR, and Special Sensor Microwave/Imager, or SSM/I) and optical remote sensing platforms (Advanced Very High Resolution Radiometer, or AVHRR) provided by the National Snow and Ice Data Center (Fowler and Tschudi, 2010). Mean vector fields were created for July to September of each year and then averaged over the period 1996–2010.

Finally, we used a helicopter-mounted electromagnetic induction system (HEMI) called IcePic™ to measure ice thickness in the southern Beaufort Sea. (See Kovacs and Holladay, 1990 or Peterson et al., 2008 for detailed information on this system, and Haas et al., 1997, 2010; Haas, 1998, 2004 for its methodology and uncertainties.) The system works by measuring the distance from the helicopter to the ice-seawater interface via electromagnetic induction and the distance from the helicopter to the ice surface using laser altimetry. The difference between those two distances represents the ice thickness. The system acquires electromagnetic induction and laser data at 10 Hz, so the spatial sampling interval in a straight line is 4–5 m (Peterson et al., 2008). When the HEMI system is flown over open water, the altimeter fails because the laser beam is absorbed by the surface. Those records are removed from the dataset in the quality control phase, so that all HEMI data unambiguously represent measurements of sea ice thickness. The HEMI system has an upper measurable limit of sea ice thickness because of a limitation in the range of the electromagnetic induction system. Ice thickness that exceeds this limit (estimated to be ~10 m at typical flight altitudes) cannot be determined.

HEMI data were collected between 31 August and 10 September 2009 from the CCGS *Amundsen* using the ship's BO-105 helicopter as weather allowed in the vicinity (~75 km) of oceanographic stations sampled as part of a multidisciplinary ArcticNet science cruise. The flight patterns were chosen using the previous days' RADARSAT-1 imagery provided to the CCGS *Amundsen*. In combination with similar data collected in the southern Beaufort Sea by Haas et al. (2010) in April 2009, this dataset can be used to provide a unique characterization of ice thickness during a summer drilling season. We presume that sea ice thickness of the region varies from year to year (e.g., Haas and Eicken, 2001); however, since sea ice thickness data were available for both April and September of 2009, we use that year as a case study.

## RESULTS

### *Summer Sea Ice Extent*

In summer in the southern Beaufort Sea, a transition zone of increasing ice concentrations occurs between the open ocean (nearest the continental coast, Banks Island, and Amundsen Gulf) and core Beaufort Sea high ice concentrations (9–10 tenths), which begin at about 73.5° N (Fig. 1a). Between 1996 and 2010, areas where oil exploration leases currently exist near the Mackenzie delta experienced 0 to 5 tenths total sea ice concentration, and on average, most of the ice cover in the area was old ice (Fig. 1a, b).

In recent years, several studies have noted that the summer sea ice of the Beaufort Sea has eroded substantially in terms of thickness and extent (e.g., Perovich et al., 2008; Barber et al., 2009; Kwok et al., 2009). Linear regression analysis on the summer mean sea ice concentrations of total ice, old ice, and first-year ice elucidates trends in these sea ice stages of development between 1996 and 2010 (Fig. 2). The study region experienced a statistically significant decreasing trend in total sea ice concentration in the area east of the oil lease blocks, north of the Tuktoyaktuk Peninsula, Cape Bathurst, and Franklin Bay (Fig. 2a). Trend analysis also shows that the Beaufort Sea summer pack has experienced a statistically significant decreasing trend in old ice concentration in the northwest quadrant of the study region (Fig. 2c). These losses are lessened in the context of total ice concentration by smaller but statistically significant increasing trends in first-year sea ice concentrations (Fig. 2e). This finding corroborates the results of Maslanik et al. (2011), who show that sea ice in the Arctic has gotten younger in recent years. Importantly, the ocean areas occupied by the current oil exploration leases near the Mackenzie Delta have experienced no significant trends in summer total, old, or first-year sea ice between 1996 and 2010.

These regional trends are apparent in the mean summer sea ice cover in 2009 (Fig. 3a), which illustrates the erosion of summer old sea ice (Fig. 3b) in the southern Beaufort Sea with respect to the longer term mean (Fig. 1b)

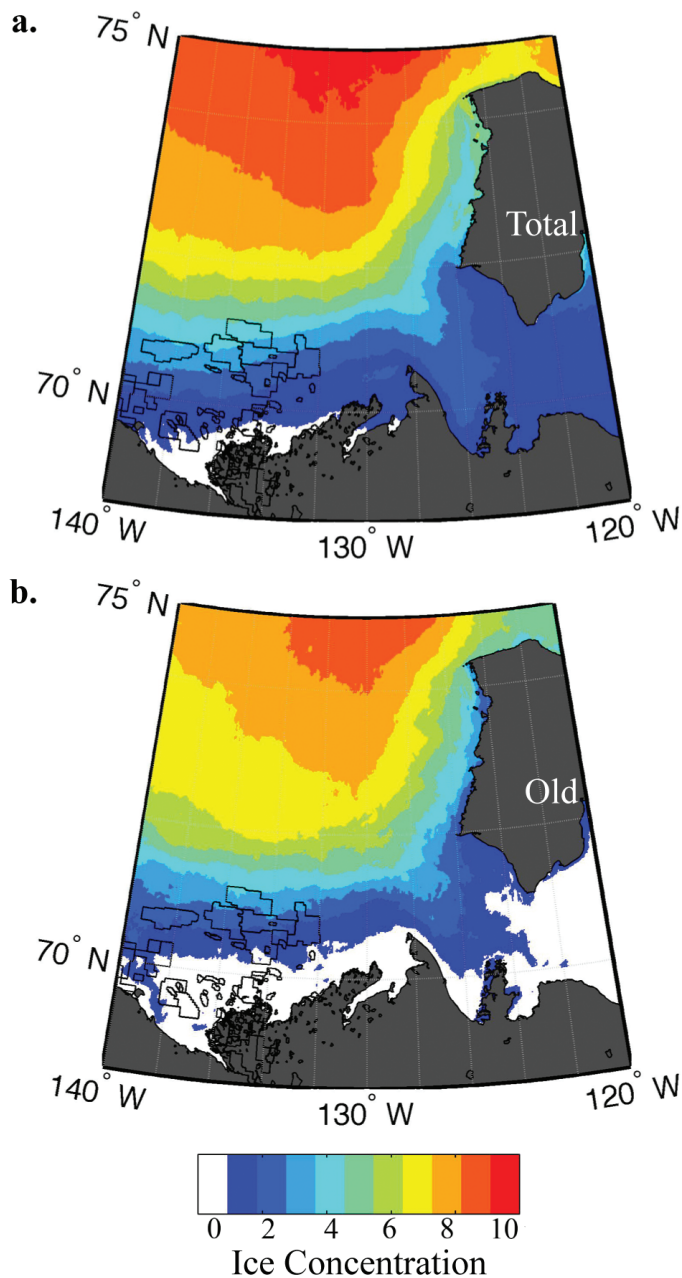


FIG. 1. Mean summer (July to September) concentrations of (a) total sea ice and (b) old sea ice, 1996–2010 (in tenths). Black polygons indicate areas of oil exploration licenses.

and its replacement (in part) by first-year sea ice (Fig. 2e, f). In summer 2009, the area of high (9–10 tenths) historical sea ice concentrations (Fig. 1a) contained less old sea ice (Fig. 3b) compared to the longer-term average (Fig. 1b). However, many of the exploration lease areas contained a greater concentration of total sea ice (Fig. 3a) even though old ice was much less prevalent in the region (Fig. 3b) in summer 2009. These results show that variability in the exposure of offshore equipment to old sea ice floes in summer could depend on differences in just tens of kilometers. Analysis of monthly means for both the long term (1996–2010) and 2009 (not shown) reveals that the largest differences from the long-term mean concentration and

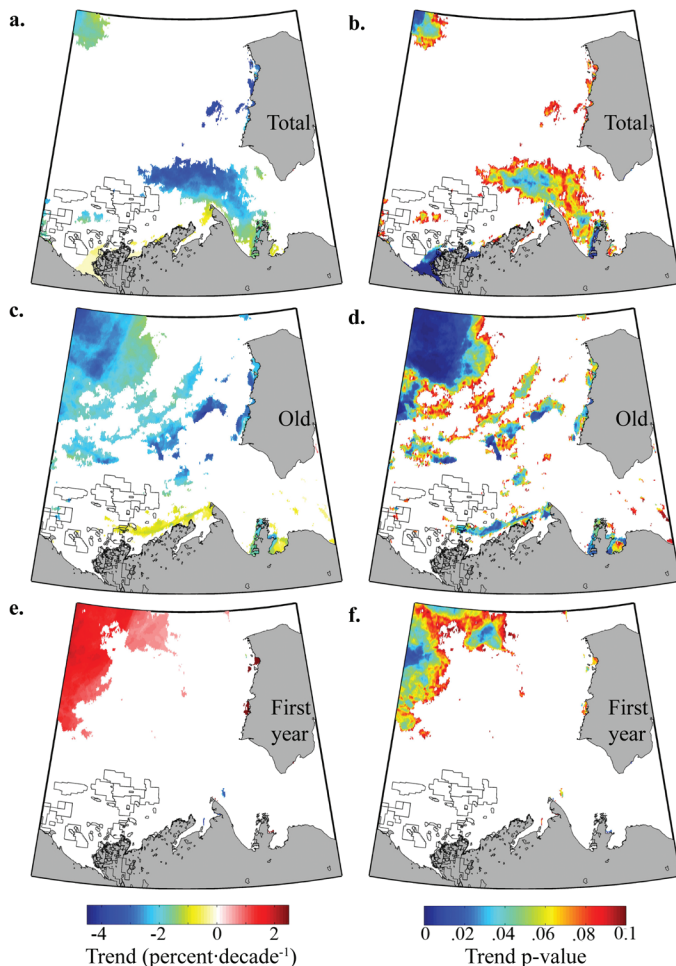


FIG. 2. Linear trends for sea ice concentrations in the Beaufort Sea for (a, b) total ice, (c, d) old ice, and (e, f) first-year ice, 1996–2010. Left column shows percent change per decade, and right column, associated *p*-values.

extent in the southern Beaufort Sea occurred in July. That is, in 2009 most of the sea ice loss occurred early in the summer drilling season (July), as similarly reported for summer 2007 by Perovich et al. (2008), especially in ice-edge (peripheral) areas that include the oil lease regions.

### Sea Ice Motion

Average summer sea ice motion in the study area (Fig. 4a) indicates predominantly anti-cyclonic (clockwise) circulation during the period 1996–2010. On average, sea ice is transported eastward in the northern reaches of the Beaufort Gyre, then southward down the western coast of the Canadian Arctic Archipelago along the Parry Islands, across M’Clure Strait, and finally along the west coast of Banks Island before it turns west, following the northern continental coast and crossing the mouth of the Mackenzie River (Fig. 4a). The mean summer sea ice velocity in the southern Beaufort Sea between 1996 and 2010 was less than 25 cm·s<sup>-1</sup> west of M’Clure Strait at its maximum, slowing slightly (to 15 cm·s<sup>-1</sup>) as it turned southwest and then west outside the mouth of Amundsen Gulf (Fig. 4a).

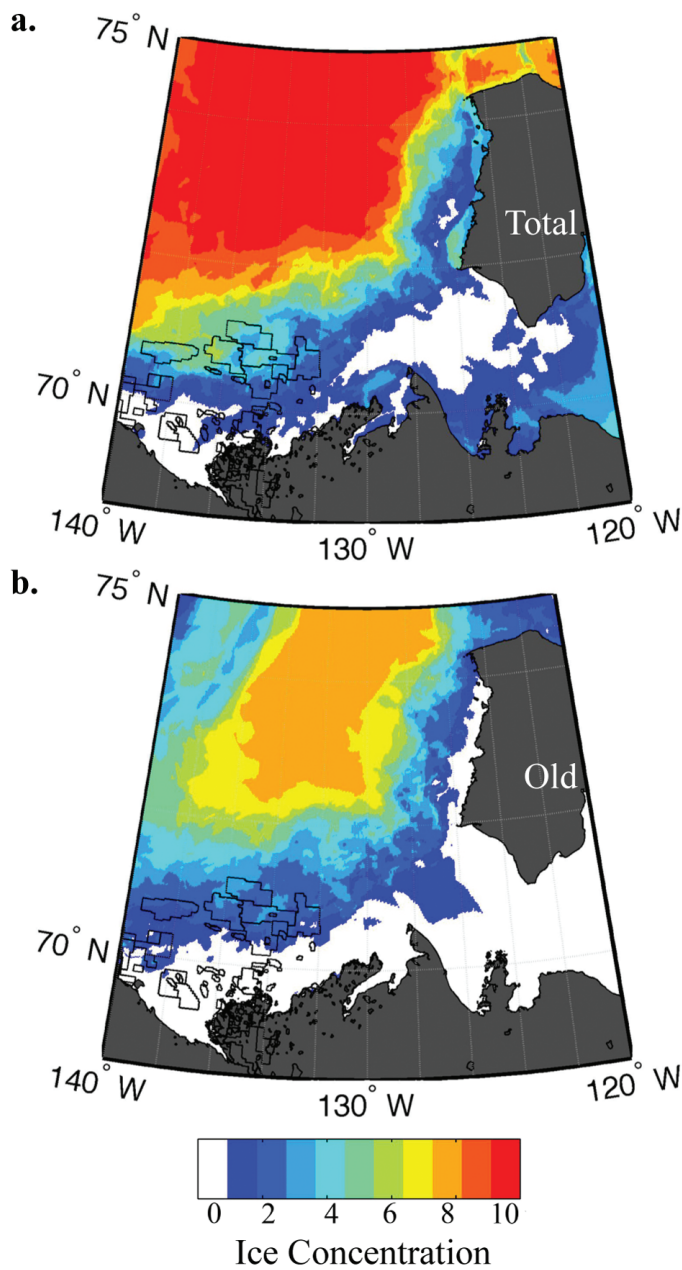


FIG. 3. Mean concentrations of (a) total sea ice and (b) old sea ice for July to September 2009 (in tenths).

In the summer of 2009, the pronounced anti-cyclonic sea ice motion was geographically similar to the 1996–2010 average (Fig. 4a), but the average sea ice velocity was much higher (Fig. 4b). In 2009, two areas of maximum velocity ( $55$  to  $60$   $\text{cm}\cdot\text{s}^{-1}$ ) occurred: one along the west coast of Banks Island and the second along the northern continental coast west of the mouth of the Mackenzie River (Fig. 4b). In 2009, the center of the Beaufort Gyre (Fig. 4b) was about  $90$  km northwest of its average (1996–2010) position (Fig. 4a), and the area with near-zero sea ice velocities expanded farther to the northwest (Fig. 4).

In the context of the Canadian oil exploration leases offshore of the Mackenzie River delta, the prevailing circulation (Fig. 4) acts to transport the high-concentration

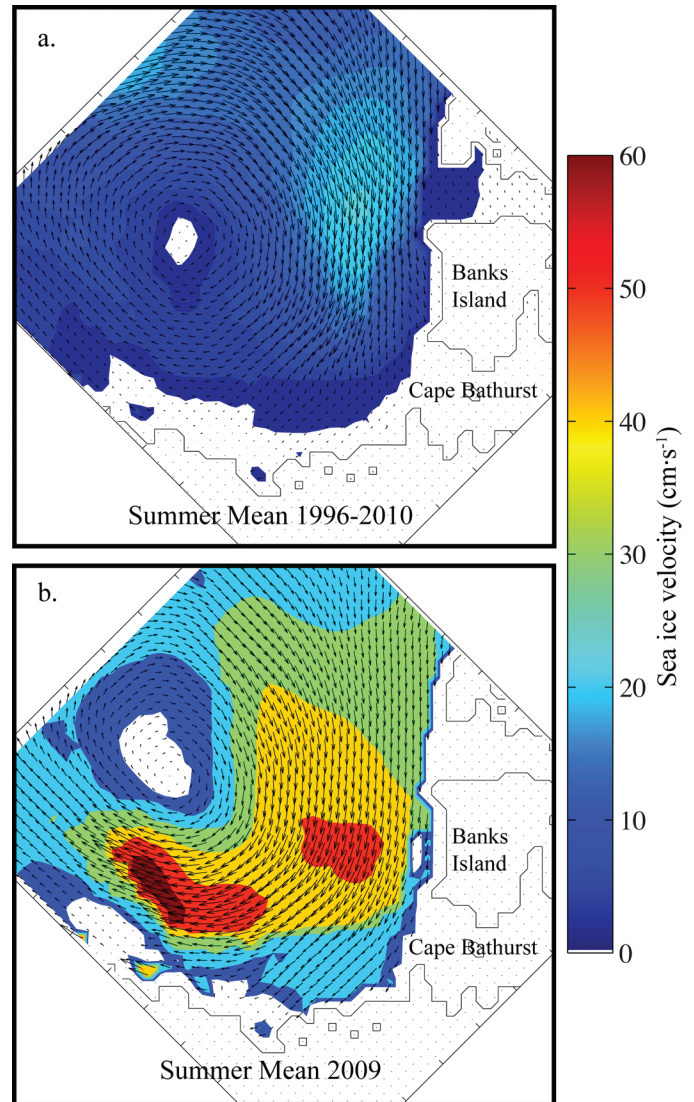


FIG. 4. Mean summer (July to September) sea ice motion ( $\text{cm}\cdot\text{s}^{-1}$ ) in the southern Beaufort Sea for (a) 1996–2010 and (b) 2009.

Beaufort Sea pack ice (Figs. 1, 3) south toward the lease areas and west across the mouth of the Mackenzie River. Since summer ice concentrations increase northward and contain predominantly old ice, this circulation pattern acts to maintain ice concentrations in the lease areas. This southward transport (Fig. 4) represents a continuous influx of thick ice (Figs. 1 and 3 and see, for example, Haas et al., 2010). Further, the northwest flank of the Canadian Arctic Archipelago is a source of ice islands, which may be entrained in the Beaufort Sea gyre and advected southward towards the lease blocks in the southern Beaufort Sea (e.g., Sackinger et al., 1991). Back-of-the-envelope calculations indicate that southward motion during summer at the long-term average velocity of  $25$   $\text{cm}\cdot\text{s}^{-1}$  can move sea ice from the mouth of McClure Strait north of Banks Island to Cape Bathurst ( $\sim 5^\circ$  latitude or  $\sim 550$  km) in 25 days. However, at velocities of  $60$   $\text{cm}\cdot\text{s}^{-1}$ , sea ice floes can cover the same distance in less than 11 days.

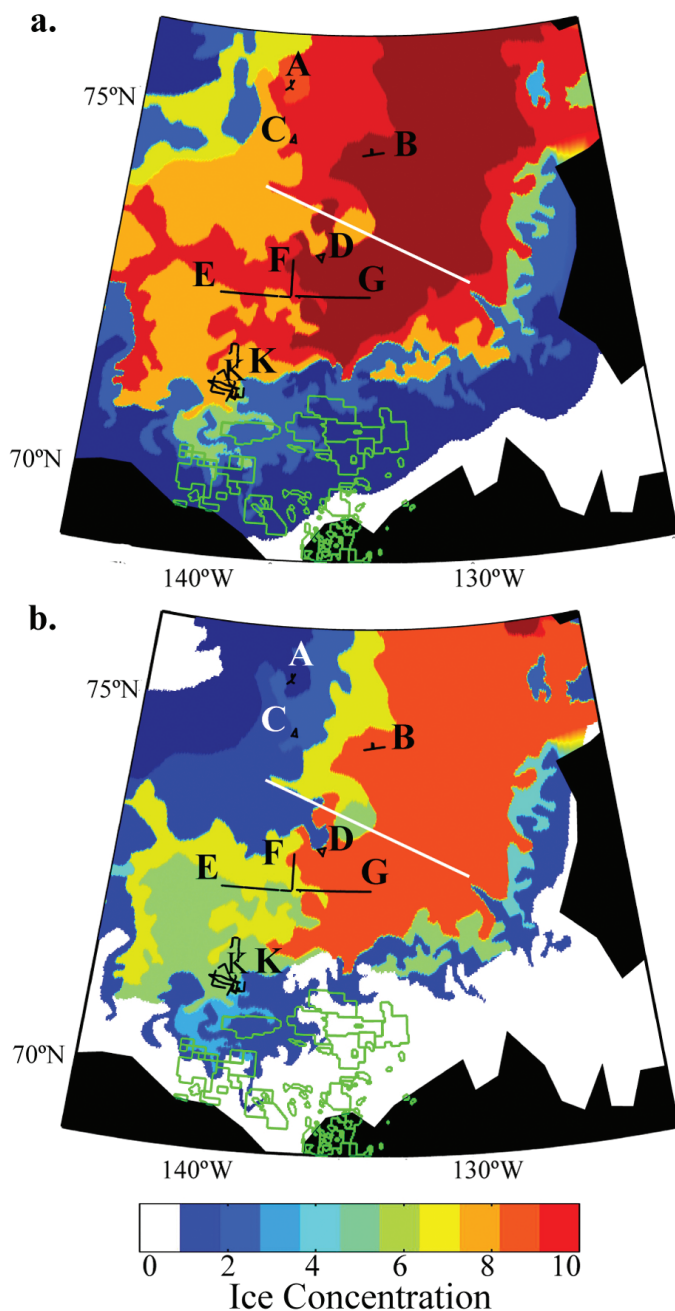


FIG. 5. Sea ice thickness locations (black lines) from the helicopter electromagnetic induction (HEMI) system in the southern Beaufort Sea, 31 August to 10 September 2009, superimposed on Canadian Ice Service concentrations for (a) total ice and (b) old sea ice from 07 Sep 2009 (colorbar). Letters indicate our September flights, the white line shows the approximate April 2009 flight path of Haas et al. (2010), and green polygons indicate Canadian oil exploration license areas. See Table 1 for details from each flight.

#### *Sea Ice Thickness in the Beaufort Sea in 2009*

The dates and ice thicknesses of the HEMI system IcePic flights are shown in Table 1, and their locations are shown by the letters in Figure 5. These locations are superimposed on the CIS chart data for total sea ice concentration (Fig. 5a) and old sea ice concentration (Fig. 5b) from 7 September 2009. Table 1 contains pertinent information and

summary statistics for each flight, the total and partial sea ice concentrations, and the percentages of the cumulative distribution with thickness less than 0.50 m, 1.00 m, and 2.00 m. The flights were conducted over a range of ice concentrations and ice thicknesses, effectively capturing conditions in the middle of the multi-year ice core west of Banks Island and along the periphery of that feature (Fig. 5). Qualitatively, sea ice in the Beaufort Sea at that time was lightly snow covered and free of unfrozen melt ponds in the north and free of snow with frozen melt ponds in the south. Thaw holes existed in some floes in the study area.

The sea ice thickness histogram for all the fall 2009 flight data is shown in Figure 6a, and is accompanied by their cumulative distribution function (CDF) (Fig. 6b). All thickness histograms and CDFs shown herein contain thickness bins 0.10 m wide beginning at 0.00 m. The mean sea ice thickness in fall 2009 was 1.03 m ( $\sigma = 0.97$  m) (Table 1). The sea ice thickness histogram of all the fall data is roughly unimodal about the 0.20–0.29 m thickness bin, with a right tail showing approximately exponentially decreasing ( $\sim e^{-x}$ ) occurrence values (Fig. 6a). The CDF reveals that 35% of the sea ice sampled was less than 0.50 m thick, 62.7% was less than 1.0 m thick, 23% was between 1.0 m and 1.99 m thick, 9% was between 2.0 m and 3.0 m thick, and 4.2% was more than 3.0 m thick (Fig. 6b). The far-right end of the percent occurrence histogram shows that some very thick ( $> 4$  m) ridged sea ice occurred in the region, including some ridges thicker than the 10 m measurement limit of the HEMI system (Fig. 6a; see METHODS).

This sea ice thickness distribution histogram in the southern Beaufort Sea for 31 August to 10 September 2009 is especially interesting in the context of the southern Beaufort Sea ice thickness data presented by Haas et al. (2010). The approximate location of the flight over the Beaufort Sea undertaken by Haas et al. (2010) in April 2009 is shown on Figure 5 (white line). Histogram 6 in Figure 1 of Haas et al. (2010) shows the distribution of sea ice thickness obtained from flight legs (total distance = 426 km) across the southern Beaufort Sea from Sachs Harbour in a west-northwest direction on 16 April 2009. The party encountered the thickest sea ice in the middle 200 km of their flight west of Banks Island and thinner first year ice (mean thickness 1.69 m) once they passed the western edge of the high concentration multi-year ice core (Haas et al., 2010). The April 2009 sea ice thickness distribution was roughly bimodal, with peaks in the distribution at about 0.8 m (caused by relatively young or medium first-year ice) and at 2.1 m (caused by older, thick first-year ice; Haas et al., 2010). The authors also observed a weak third mode around 3.2 m, which was likely caused by multi-year ice, and an extended right tail signifying the presence of pressure ridges. A comparison of the April distribution of Haas et al. (2010) to our sea ice thickness distributions (Fig. 6a, Table 1) shows that the thin sea ice ( $< 1.0$  m) mode in April in the region was not present in September 2009 and the April mode at 2.10 m was replaced in September by a mode around 0.60 m (Fig. 6a). Predominantly thinner ice was also apparent in

TABLE 1. HEMI flight sea ice thickness statistics and their respective sea ice concentrations (from CIS digital data) in the southern Beaufort Sea in 2009.

Flight	Date	km	Points	Mode (m-bin)	Mean (m)	SD	Ice Concentration (10ths)		Cumulative distribution (%)		
							Total	Partial	< 0.50 m	< 1.00 m	< 2.00 m
A	07 September	23.5	3737	0.10–0.19	0.49	0.63	8	0.3 Old, 8 Thick FY	65	88	98
B	06 September	46.5	10861	0.90–0.99	1.89	1.2	9.7	8 Old, 2 Thick FY	6	25	61
C	04 September	32	7443	0.20–0.29	0.65	0.68	9	2 Old, 7 Thick FY	55	83	95
D	08 September	35.3	7196	0.20–0.29	0.7	0.87	9	6 Old, 3 Thick FY	56	82	95
E	09 September	102.5	21809	0.20–0.29	0.77	0.76	7	5 Old, 2 Thick FY	47	78	93
F	10 September	52	10730	0.50–0.59	0.86	0.65	9	6 Old, 3 Thick FY	30	72	94
G	09 September	109	28502	0.50–0.59	1.08	0.83	9(9.7)	6(8) Old, 3(2) Thick FY	23	60	87
K	31 August–2 September	340	60374	0.00–0.09	1.09	1.04	7	5 Old, 2 Thick FY	36	58	83
<b>All</b>		<b>740.8</b>	<b>150652</b>	<b>0.20–0.29</b>	<b>1.03</b>	<b>0.97</b>			<b>35</b>	<b>62.7</b>	<b>86</b>

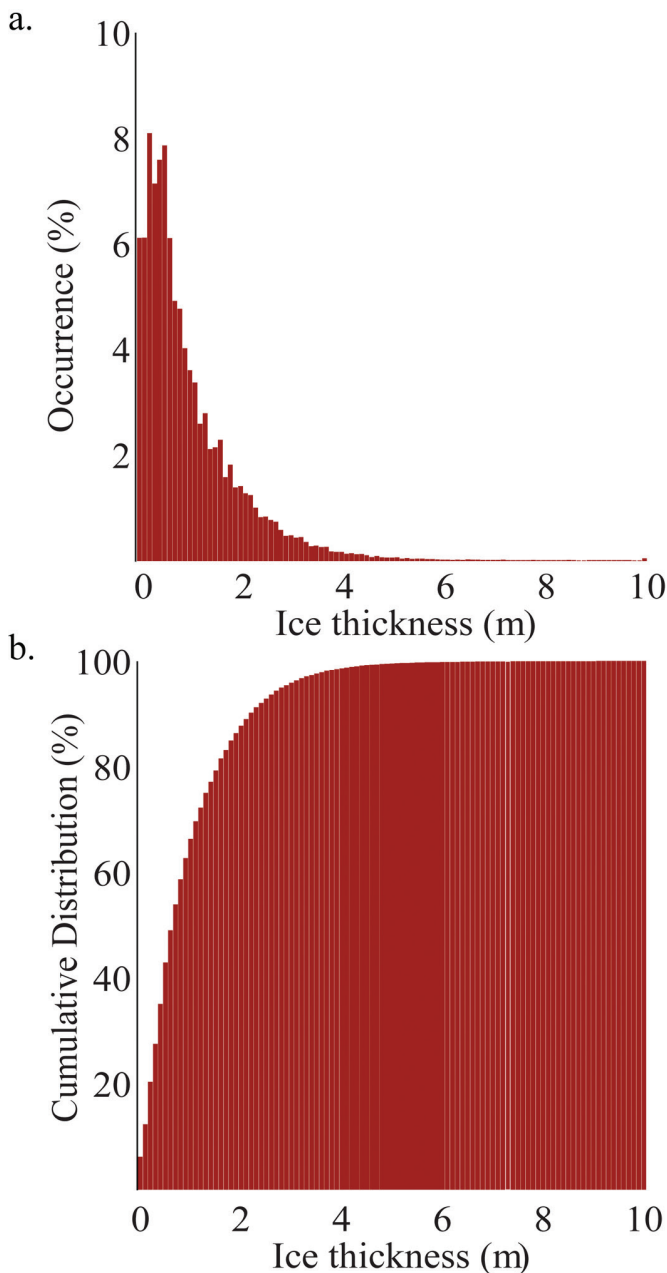


FIG. 6. (a) Frequency distribution histogram (bin width = 0.10 m) of the ice thickness data (flight locations shown in Fig. 4), where mean  $Z_i = 1.03$  m,  $\sigma = 0.97$  m, and  $n = 150652$ . (b) Cumulative distribution function (bin width = 0.10 m) of the ice thickness data collected in 2009.

the differences between mean thicknesses measured in April and September of 2009; on average, we observed sea ice that was 1–2 m thinner than that reported by Haas et al. (2010), as well as the loss of the spring sea ice mode to the left of the 1.0 m thickness bin (Fig. 6a). We compared the means of the most similar sea ice regimes observed in the core (high-concentration) multi-year drift stream of the Beaufort Sea in April 2009 (Haas et al., 2010) and during our September 2009 flights. We found that the April ice thickness means (3.08 m and 3.27 m) were 1.19 m and 1.38 m greater than the September mean (1.89 m) for sea ice observed during our flight B. In the periphery of the Beaufort Sea pack, the westernmost flight section of Haas et al. (2010) (mean = 2.33 m) is best compared geographically to either our flight C (mean = 0.65 m) or our flight E (mean = 0.77 m), showing a change in mean thickness from April to September of 1.68 m or 1.56 m, respectively. It is difficult to infer ice melt from these results, given that our flights would not have sampled the same floes as Haas et al. (2010) because of ice drift. It is interesting to compare the results of Perovich et al. (2008), who used an ice mass balance buoy to show that a multi-year sea ice floe in this region lost more than 2 m of thickness between July and September (inclusive) in 2007. Perovich et al. (2008) attribute the sea ice thickness loss they measured in the Beaufort Sea to bottom melt created by the sea ice–albedo feedback mechanism as it related to hemispheric sea ice concentration loss that summer. In the Beaufort Sea ice pack, Maslanik et al. (2011) show that older (3rd, 4th, and 5th year) ice was predominant in both May and September 2009.

Very thick sea ice in the study area at the beginning of September 2009 comprised a small percentage of the thickness distribution (Fig. 6a, b). Data collected in late August and early September 2009 indicate that only 4.2% of the ice was more than 3 m thick, and less than 1.5% was more than 4 m thick (Fig. 6b). However, the presence of even a small percentage of thick ice is significant for oil and gas development and should be considered by operators in the region.

Because of variability in the total ice concentration (and partial concentrations of old and first-year sea ice) in the region where our HEMI sea ice thickness data were collected (Fig. 5a, b), it makes sense to discuss these data in the context of their total and old sea ice concentration regimes in early September 2009. For a general perspective, all the

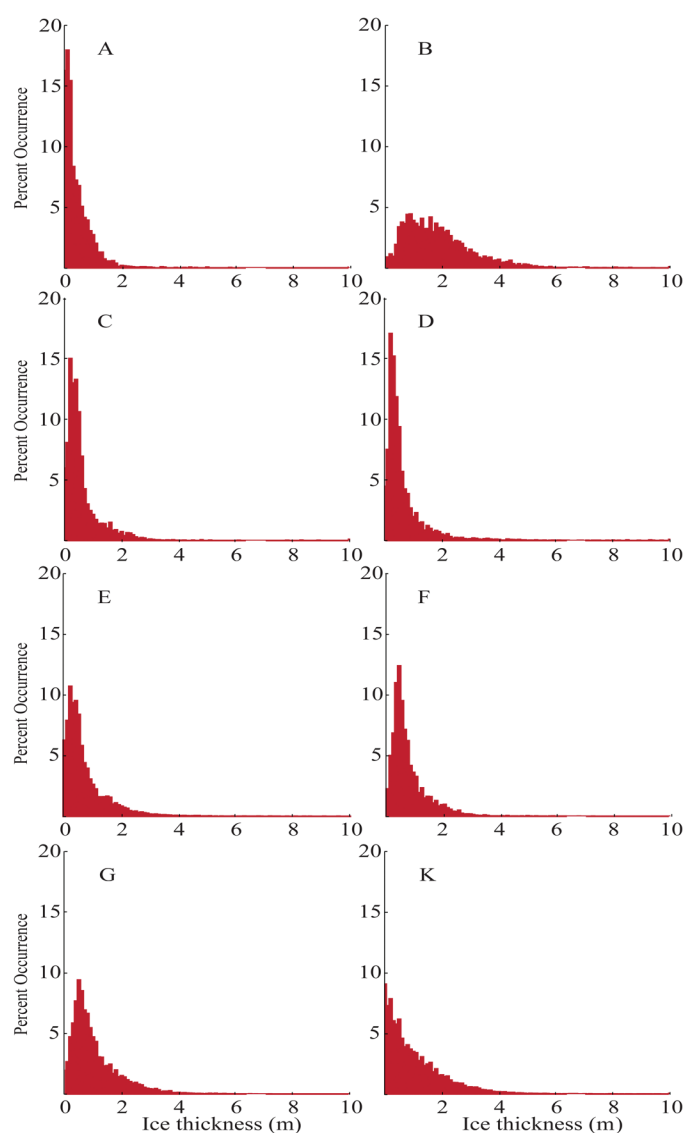


FIG. 7. Sea ice thickness distributions (bin width = 0.10 m) for individual flights mapped in Figure 5 (see Table 1 for sea ice concentration information in the flight areas).

flights were mapped on the CIS digital data for 7 September 2009 (Fig. 5). For the specific discussion of each flight that follows, the sea ice thickness distribution was compared to the CIS daily Beaufort Sea digital chart created using RADARSAT data gathered on the same date. The length of each flight, the number of sample points, mean sea ice thickness and standard deviation, sea ice concentration for the date, and cumulative distribution statistics for each flight are contained in Table 1.

The thickest ice (> 8 tenths concentration) was encountered in the northern core of the Beaufort Sea multi-year drift stream during Flight B (Fig. 5a). Ice encountered by Flights A and C, in the periphery of the Beaufort Sea pack at the north end of the study area, had much lower mean and modal thickness, with little sea ice more than 2 m thick (Table 1, Fig. 7), probably for lack of old sea ice (Fig. 5b). In the middle of the study region (~ 72.5° N; Fig. 5b), moving

from areas of lower old ice concentration (Flights D, E) to areas of higher old ice concentration (Flights F, G) reveals progressively thicker mean (Table 1) and modal (Fig. 7) ice thickness concurrent with decreasing occurrence of new and thin stages of sea ice development. At the south end of the study region, Flight K is interesting because it found a relatively large proportion (17%) of ice more than 2 m thick and a relatively small proportion (58%) of ice less than 1 m thick (Table 1). In comparison to the histogram of flight G to the north (Fig. 7G), the histogram of flight K (Fig. 7K) appears to have shifted to the left, the ice having melted as it drifted southward in the Beaufort Sea. The sea ice distribution in the southern reaches of the region (Fig. 7K, Table 1) maintains a large proportion of relatively thick sea ice because melt eliminates thinner floes from the distribution and moves thicker floes to the left within the histogram. For example, if two floes with initial thicknesses of 1.0 m and 3.0 m enter the region and both lose 1.0 m of thickness, then what remains is one floe 2.0 m thick. The sea ice thickness distribution from Flight K (Fig. 7K) shows that sea ice transported south from the northern reaches of the southern Beaufort Sea (Fig. 4) retained a relatively high fraction of thick ice likely to survive continued melt as it drifts towards the lease areas.

## CONCLUSIONS

Mean total summer sea ice concentration is decreasing in parts of the southern Beaufort Sea, a situation created by the confluence of substantially decreasing old ice concentrations and marginally increasing first-year ice concentrations in those areas, particularly in the northwest corner of our study region. Although comparison of the 2009 and 1996–2010 data in the region revealed that concentrations were lower in 2009 than over the long term, no statistically significant decreasing trends in summer sea ice concentration (for either total, old, or first-year sea ice) were seen in the oil exploration lease areas north of the Mackenzie River delta between 1996 and 2010. Oil exploration lease areas in the southern Beaufort Sea were affected by sea ice, including old ice, both on average (1996–2010) and in 2009. This effect could be due in part to wide interannual variability, or to the predominant pattern of ice circulation that moves ice from high-concentration regions to the north into the southern lease areas each summer. In 2009, the average anti-cyclonic sea ice motion of the Beaufort Sea summer pack occurred, but at velocities much greater than the longer-term average.

Data collected in the southern Beaufort Sea between 31 August and 10 September 2009 indicated a mean sea ice thickness of 1.03 m ( $\sigma = 0.97$  m) and a mode around the 0.20 to 0.29 m thickness bin. Occurrence histograms for eight flights revealed that the sea ice thickness distribution in the region in September 2009 was spatially variable; the thickest ice occurred at the northern end of our study area in an area dominated by high concentrations of old sea

ice. Thinner sea ice was more prevalent at the periphery of the core Beaufort Sea multi-year pack. At the south end of the study area, nearest the oil exploration lease areas, the sea ice thickness distribution had shifted left with respect to distributions in the north (viewed as the source area of sea ice in the south) in both April and September 2009. The southernmost sea ice thickness distribution in September contained a greater proportion of relatively thick sea ice than distributions from all the flight data from the north except Flight B. This finding led us to conclude that thin (~1.5 m or thinner) sea ice occurring farther north had melted by the time it reached the very south end of the study region. In comparison to sea ice thickness data from ~426 km flown on 16 April 2009 in the same region (Haas et al., 2010), our September data reveal a summer decrease in the mean thickness of sea ice in the Beaufort Sea of 0.44 to 2.57 m, depending on the means compared. Although sea ice in and around the oil exploration lease areas in September is present in low-to-medium concentrations, our data show that 42% of the ice that remains that far south in the Beaufort in September was thicker than 1.00 m.

#### ACKNOWLEDGEMENTS

The authors thank Chuck Fowler for providing the sea ice motion dataset and for answering questions so freely. The authors extend their thanks and appreciation to Canadian Coast Guard pilot Guillaume Carpentier for his skill and professionalism in flying and pleasant conversation. Thanks to the Canadian Ice Service for making the CISDA freely available. The authors acknowledge financial support from ArcticNet's industry partners, including Imperial Oil Ltd. and BP. Thanks to the Natural Sciences and Engineering Research Council, the ArcticNet Network of Centres of Excellence program, and the Canada Research Chairs program for grants to D.G. Barber. B.G.T. Else is supported by a Vanier Canada graduate scholarship.

#### REFERENCES

- ArcticNet. 2009. Coming together in the study of a changing Canadian Arctic. Annual Report 2007–2009. Quebec City: ArcticNet Inc., Université Laval. <http://www.arcticnet.ulaval.ca/media/annualreport.php>. 128 p.
- Asplin, M.A., Lukovich, J.V., and Barber, D.G. 2009. Atmospheric forcing of the Beaufort Sea ice gyre: Surface pressure climatology and sea ice motion. *Journal of Geophysical Research* 114, C00A06, doi:10.1029/2008JC005127.
- Barber, D.G., Galley, R., Asplin, M.G., De Abreu, R., Warner, K.-A., Pucko, M., Gupta, M., Prinsenberg, S., and Julien, S. 2009. Perennial pack ice in the southern Beaufort Sea was not as it appeared in the summer of 2009. *Geophysical Research Letters* 36, L24501, doi:10.1029/2009GL041434.
- Barnett, D.G. 1976. A practical method of long-range ice forecasting for the north coast of Alaska. Technical Report. Suitland, Maryland: Fleet Weather Facility. 16 p.
- . 1980. A long-range ice forecasting method for the north coast of Alaska. In: Pritchard, R.S., ed. *Sea ice processes and models: Proceedings of the Arctic Ice Dynamics Joint Experiment International Commission of Snow and Ice Symposium*. Seattle: University of Washington Press. 360–373.
- Barry, R.G., and Maslanik, J. 1989. Arctic sea ice characteristics and associated atmosphere-ice interactions in summer inferred from SMMR data and drifting buoys: 1979–1984. *GeoJournal* 18(1):35–44.
- CIS (Canadian Ice Service). 2010. *Sea ice climatic atlas for the northern Canadian waters 1981–2010*. Ottawa: Environment Canada. 995 p.
- Colony, R., and Thorndike, A.S. 1984. An estimate of the mean field of Arctic sea ice motion. *Journal of Geophysical Research* 89(C6):10623–10629, doi:10.1029/JC089iC06p10623.
- Comiso, J.C. 2002. A rapidly declining perennial sea ice cover in the Arctic. *Geophysical Research Letters* 29, 1956, doi:10.1029/2002GL015650.
- Comiso, J.C., and Nishio, F. 2008. Trends in the sea ice cover using enhanced and compatible AMSR-E, SSM/I, and SMMR data. *Journal of Geophysical Research*, 113, C02S07, doi:10.1029/2007JC004257.
- Drobot, S.D., and Maslanik, J.A. 2003. Interannual variability in summer Beaufort Sea ice conditions: Relationship to winter and summer surface and atmospheric variability. *Journal of Geophysical Research* 108(C7), 3233, doi:10.1029/2002JC001537.
- Fowler, C., and Tschudi, M. 2010 (Updated from 2003). *Polar Pathfinder daily 25 km EASE-grid sea ice motion vectors*. Boulder, Colorado: National Snow and Ice Data Center. Digital media.
- Galley, R.J., Key, E., Barber, D.G., Hwang, B.-J., and Ehn, J.K. 2008. Spatial and temporal variability of sea ice in the southern Beaufort Sea and Amundsen Gulf: 1980–2004. *Journal of Geophysical Research* 113, C05S95, doi:10.1029/2007JC004553.
- Gautier, D.L., Bird, K.J., Charpentier, R.R., Grantz, A., Houseknecht, D.W., Klett, T.R., Moore, T.E., et al. 2009. Assessment of undiscovered oil and gas in the Arctic. *Science* 324(5931):1175–1179, doi:10.1126/science.1169467.
- Haas, C. 1998. Evaluation of ship-based electromagnetic-inductive thickness measurements of summer sea-ice in the Bellingshausen and Amundsen Seas, Antarctica. *Cold Regions Science and Technology* 27:1–16.
- . 2004. Late-summer sea ice thickness variability in the Arctic Transpolar Drift 1991–2001 derived from ground-based electromagnetic sounding. *Geophysical Research Letters* 31, L09402, doi:10.1029/2003GL019394.
- Haas, C., and Eicken, H. 2001. Interannual variability of summer sea ice thickness in the Siberian and central Arctic under different atmospheric circulation regimes. *Journal of Geophysical Research* 106(C3):4449–4462, doi:10.1029/1999JC000088.
- Haas, C., Gerland, S., Eicken, H., and Miller, H. 1997. Comparison of sea-ice thickness measurements under summer and winter conditions in the Arctic using a small electromagnetic induction device. *Geophysics* 62(3):749–757.

- Haas, C., Hendricks, S., Eicken, H., and Herber, A. 2010. Synoptic airborne thickness surveys reveal state of Arctic sea ice cover. *Geophysical Research Letters* 37, L09501, doi:10.1029/2010GL042652.
- Kimura, N., and Wakatsuchi, M. 2000. Relationship between sea-ice motion and geostrophic wind in the Northern Hemisphere. *Geophysical Research Letters* 27(22):3735–3738, doi:10.1029/2000GL011495.
- Kovacs, A., and Holladay, J.S. 1990. Sea-ice thickness measurement using a small airborne electromagnetic sounding system. *Geophysics* 55(1):1327–1337.
- Kwok, R. 2007. Near zero replenishment of the Arctic multiyear sea ice cover at the end of 2005 summer. *Geophysical Research Letters* 34, L05501, doi:10.1029/2006GL028737.
- Kwok, R., Cunningham, G.F., Wensnahan, M., Rigor, I., Zwally, H.J., and Yi, D. 2009. Thinning and volume loss of the Arctic Ocean sea ice cover: 2003–2008. *Journal of Geophysical Research* 114, C07005, doi:10.1029/2009JC005312.
- Lukovich, J.V., and Barber, D.G. 2006. Atmospheric controls on sea ice motion in the southern Beaufort Sea. *Journal of Geophysical Research* 111, D18103, doi:10.1029/2005JD006408.
- Maslanik, J., Fowler, C., Stroeve, J., Drobot, S., Zwally, J., Yi, D., and Emery, W. 2007. A younger, thinner Arctic sea ice cover: Increased potential for rapid, extensive sea-ice loss. *Geophysical Research Letters* 34, L24501, doi:10.1029/2007GL032043.
- Maslanik, J., Stroeve, J., Fowler, C., and Emery, W. 2011. Distribution and trends in Arctic sea ice age through spring 2011. *Geophysical Research Letters* 38, L13502, doi:10.1029/2011GL047735.
- Meier, W.N., Stroeve, J., and Fetterer, F. 2007. Whither Arctic sea ice? A clear signal of decline regionally, seasonally and extending beyond the satellite record. *Annals of Glaciology* 46(1):428–434.
- Melling, H., and Riedel, D.A. 2004. Draft and movement of pack ice in the Beaufort Sea: A time-series presentation April 1990–August 1999. *Canadian Technical Report of Hydrography and Ocean Sciences* 238. Sidney, British Columbia: Institute of Ocean Sciences, Fisheries and Oceans Canada. 24 p.
- Melling, H., Riedel, D.A., and Gedalof, Z. 2005. Trends in the draft and extent of seasonal pack ice, Canadian Beaufort Sea. *Geophysical Research Letters* 32, L24501, doi:10.1029/2005GL024483.
- Moore, D.S. 1995. *The basic practice of statistics*. New York: W.H. Freeman and Company. 674 p.
- Nghiem, S.V., Chao, Y., Neumann, G., Li, P., Perovich, D.K., Street, T., and Clemente-Colón, P. 2006. Depletion of perennial sea ice in the East Arctic Ocean. *Geophysical Research Letters* 33, L17501, doi:10.1029/2006GL027198.
- Northern Oil and Gas Branch. 2009. *Northern oil and gas annual report 2008*. Ottawa: Aboriginal Affairs and Northern Development Canada. 31 p.
- Ogi, M., Rigor, I.G., McPhee, M.G., and Wallace, J.M. 2008. Summer retreat of Arctic sea ice: Role of summer winds. *Geophysical Research Letters* 35, L24701, doi:10.1029/2008GL035672.
- Overland, J.E. 2009. Meteorology of the Beaufort Sea. *Journal of Geophysical Research* 114, C00A07, doi:10.1029/2008JC004861.
- Parkinson, C.L., and Cavalieri, D.J. 2008. Arctic sea ice variability and trends, 1979–2006. *Journal of Geophysical Research* 113, C07003, doi:10.1029/2007JC004558.
- Parkinson, C.L., Cavalieri, D.J., Gloersen, P., Zwally, H.J., and Comiso, J.C. 1999. Arctic sea ice extents, areas, and trends 1978–1996. *Journal of Geophysical Research* 104(C9):20837–20856, doi:10.1029/1999JC900082.
- Perovich, D.K., and Richter-Menge, J.A. 2009. Loss of sea ice in the Arctic. *Annual Review of Marine Science* 1:417–441, doi:10.1146/annurev.marine.010908.163805.
- Perovich, D.K., Richter-Menge, J.A., Jones, K.F., and Light, B. 2008. Sunlight, water, and ice: Extreme Arctic sea ice melt during the summer of 2007. *Geophysical Research Letters* 35, L11501, doi:10.1029/2008GL034007.
- Peterson, I.K., Prinsenberg, S.J., and Holladay, J.S. 2008. Observations of sea ice thickness, surface roughness and ice motion in Amundsen Gulf. *Journal of Geophysical Research* 113, C06016, doi:10.1029/2007JC004456.
- Preller, R.H., and Posey, P.G. 1989. A numerical model simulation of a summer reversal of the Beaufort Gyre. *Geophysical Research Letters* 16(1):69–72.
- Proshutinsky, A., Bourke, R.H., and McLaughlin, F.A. 2002. The role of the Beaufort Gyre in Arctic climate variability: Seasonal to decadal climate scales. *Geophysical Research Letters* 29(23), doi:10.1029/2002GL015847.
- Rigor, I.G., Wallace, J.M., and Colony, R.L. 2002. Response of sea ice to the Arctic oscillation. *Journal of Climate* 15(18):2648–2663.
- Rothrock, D.A., Yu, Y., and Maykut, G.A. 1999. Thinning of the Arctic sea-ice cover. *Journal of Geophysical Research* 26(23):3469–3472.
- Sackinger, W.M., Jeffries, M.O., Li, F., and Lu, M. 1991. Ice island creation, drift, recurrences, mechanical properties, and interactions with Arctic offshore oil production structures. U.S. Department of Energy Report DE92 012455. Fairbanks: Geophysical Institute, University of Alaska.
- Serreze, M.C., and Barrett, A.P. 2011. Characteristics of the Beaufort Sea High. *Journal of Climate* 24(1):159–182, doi:10.1175/2010JCLI3636.1.
- Serreze, M.C., Barry, R.G., and McLaren, A.S. 1988. Reversals of the Beaufort gyre sea ice circulation and effects on ice concentration in the Canada basin. *EOS Transactions of the American Geophysical Union* 69(44):1270.
- . 1989. Seasonal variations in sea ice motion and effects on sea ice concentration in the Canada Basin. *Journal of Geophysical Research* 94(C8):10955–10970.
- Spreen, G., Kwok, R., and Menemenlis, D. 2011. Trends in Arctic sea ice drift and role of wind forcing: 1992–2009. *Geophysical Research Letters* 38, L19501, doi:10.1029/2011GL048970.
- Stroeve, J., Holland, M.M., Meier, W., Scambos, T., and Serreze, M. 2007. Arctic sea ice decline: Faster than forecast. *Geophysical Research Letters* 34, L09501, doi:10.1029/2007GL029703.

- Tivy, A., Howell, S.E.L., Alt, B., McCourt, S., Chagnon, R., Crocker, G., Carrieres, T., and Yackel, J.J. 2011. Trends and variability in summer sea ice cover in the Canadian Arctic based on the Canadian Ice Service Digital Archive, 1960–2008 and 1968–2008. *Journal of Geophysical Research* 16, C03007, doi:10.1029/2009JC005855.
- USGS World Energy Assessment Team. 2000. U.S. Geological Survey world petroleum assessment 2000 – Description and results: U.S. Geological Survey Digital Data Series, DDS-60. <http://pubs.usgs.gov/dds/dds-060/>.
- Vowinckel, E., and Orvig, S. 1970. The climate of the North Polar Basin. In: Orvig, S., ed. *Climates of the Polar regions, World survey of climatology*, Vol. 14. Amsterdam: Elsevier Publishing Company. 283–299.
- Yu, Y., Maykut, G.A., and Rothrock, D.A. 2004. Changes in the thickness distribution of Arctic sea ice between 1958–1970 and 1993–1997. *Journal of Geophysical Research* 109, C08004, doi:10.1029/2003JC001982.